



**HAL**  
open science

**Analysis of the potential and limitations of microwave radiometry for the retrieval of sea surface temperature: Definition of MICROWAT, a new mission concept**

C. Prigent, F. Aires, Frédéric Bernardo, J.-C. Orlhac, J.-M. Goutoule, H. Roquet, C. Donlon

► **To cite this version:**

C. Prigent, F. Aires, Frédéric Bernardo, J.-C. Orlhac, J.-M. Goutoule, et al.. Analysis of the potential and limitations of microwave radiometry for the retrieval of sea surface temperature: Definition of MICROWAT, a new mission concept. *Journal of Geophysical Research. Oceans*, 2013, 118 (6), pp.3074-3086. 10.1002/jgrc.20222 . hal-02524064

**HAL Id: hal-02524064**

**<https://hal.science/hal-02524064>**

Submitted on 8 Oct 2021

**HAL** is a multi-disciplinary open access archive for the deposit and dissemination of scientific research documents, whether they are published or not. The documents may come from teaching and research institutions in France or abroad, or from public or private research centers.

L'archive ouverte pluridisciplinaire **HAL**, est destinée au dépôt et à la diffusion de documents scientifiques de niveau recherche, publiés ou non, émanant des établissements d'enseignement et de recherche français ou étrangers, des laboratoires publics ou privés.

Copyright

# Analysis of the potential and limitations of microwave radiometry for the retrieval of sea surface temperature: Definition of MICROWAT, a new mission concept

C. Prigent,<sup>1</sup> F. Aires,<sup>2,3</sup> F. Bernardo,<sup>2</sup> J.-C. Orlhac,<sup>4</sup> J.-M. Goutoule,<sup>4</sup> H. Roquet,<sup>5</sup> and C. Donlon<sup>6</sup>

Received 28 January 2013; revised 24 April 2013; accepted 27 April 2013; published 19 June 2013.

[1] The sensitivity of passive microwave observations to the sea surface temperature (SST) is carefully analyzed, with the objective of designing an optimized satellite instrument, MICROWave Wind And Temperature (MICROWAT), dedicated to an “all-weather” estimation of the SST at high spatial resolution (15 km). Our study stresses the importance of low-frequency observations around 6 GHz for accurate SST retrieval. Compared to the 11 GHz channel, the 6 GHz channel provides more sensitivity to the low SSTs and offers lower instrument noise, thanks to possibly broader channel bandwidths. However, it requires much larger antenna size for a given spatial resolution. Two instrument concepts have been suggested, one using a classic real aperture antenna and the other using synthetic interferometric antennas. This first analysis shows that 2-D interferometric systems would be very complex and would not satisfy the user requirements in terms of SST accuracy. A 1-D interferometric system could be proposed, but its development requires additional investigation. A dedicated conical scanner onboard a microsatellite with a 6 m antenna and channels at 6.9 and 18.7 GHz (both with V and H polarizations) can provide an SST accuracy of 0.3 K with a 15 km spatial resolution, with today’s technology.

**Citation:** Prigent, C., F. Aires, F. Bernardo, J.-C. Orlhac, J.-M. Goutoule, H. Roquet, and C. Donlon (2013), Analysis of the potential and limitations of microwave radiometry for the retrieval of sea surface temperature: Definition of MICROWAT, a new mission concept, *J. Geophys. Res. Oceans*, 118, 3074–3086, doi:10.1002/jgrc.20222.

## 1. Introduction

[2] The requirements of the user community for sea surface temperature (SST) are very demanding, in terms of accuracy, spatial resolution, and revisiting time. A position paper has been produced by an expert group, convened by European organisation for the Exploitation of Meteorological Satellites (EUMETSAT), in the framework of its preparatory activities for the post-European Polar Satellite (post-EPS) program [Stammer *et al.*, 2007]. It covers five application areas: oceanography (global and coastal), numerical weather prediction (NWP; global and regional), seasonal to interannual forecasting, nowcasting, and climate. The requirements are summarized in Table 1. These requirements are clearly not met by in situ measurements

provided by ships and buoys, but they are not satisfied by the current satellite observing system either.

[3] SSTs are derived from satellite infrared (IR) measurements, with high spatial resolution from polar (~1 km) or geostationary (~5 km) orbits, possibly with high temporal sampling from geostationary orbits. However, no information is provided under cloudy conditions, and, on a global basis, IR-derived SSTs only cover ~30% of the ocean per day. IR retrieval of SST is also sensitive to aerosol contamination and water vapor correction.

[4] The potential of satellite passive microwave observations to estimate SST under clouds, has been tested early, using low frequencies [e.g., *Wilheit and Chang*, 1980; *Wilheit et al.*, 1980; *Wentz et al.*, 2000]. Below 12 GHz, the passive microwave observations are proportional to the surface temperature within the first ~1 mm of the surface. The signal is little affected by atmosphere (gas, clouds, aerosols), except under rainy conditions: the lower the frequency, the lower the sensitivity to the atmosphere. In terms of spatial resolution, however, the higher the frequency, the higher the spatial resolution for a given antenna size. The signal is highly sensitive to wind-induced roughness and possible presence of foam, and these effects have to be accounted for in the retrieval. Above 5 GHz, sensitivity to salinity is limited, although some effects have been recently evidenced in the plume of large rivers [Reul *et al.*, 2009]. Ships and buoys measure the sea temperature at a depth between few tenths of meters to few meters depth

<sup>1</sup>CNRS, Laboratoire d’Etudes du Rayonnement et de la Matière en Astrophysique, Observatoire de Paris, France.

<sup>2</sup>Estellus, Paris, France.

<sup>3</sup>Laboratoire d’Etudes du Rayonnement et de la Matière en Astrophysique, Observatoire de Paris, France.

<sup>4</sup>EADS ASTRIUM France, Toulouse, France.

<sup>5</sup>Centre de Météorologie Spatiale, Météo-France, Lannion, France.

<sup>6</sup>European Space Agency, ESTEC, Noordwijk, Netherlands.

Corresponding author: C. Prigent, CNRS, Laboratoire d’Etudes du Rayonnement et de la Matière en Astrophysique, Observatoire de Paris, 61, av. de l’Observatoire, 75014 Paris, France. (catherine.prigent@obspm.fr)

**Table 1.** User Requirements for Sea Surface Temperature (SST) From *Stammer et al.* [2007]<sup>a</sup>

Applications	Accuracy (K)			Spatial resolution (km)			Revisit time (hr)		
	T	B	O	T	B	O	T	B	O
NWP global	1.5	0.5	0.3	250	15	5	120	24	3
NWP regional	1.5	1.0	0.5	50	10	1	24	6	1
NWP seasonal and interannual	0.5	0.2	0.1	50	20	1	48	12	1
Oceanography global	0.5	0.4	0.1	50	10	1	120	48	3
Oceanography costal	1.0	0.3	0.1	10	1	0.1	120	24	3

<sup>a</sup>T indicates Threshold, B Breakthrough, and O Objective values. Accuracy is the root-mean-square difference of the actual measurements and the truth, inclusive of random errors and bias.

below the surface that is free from diurnal variation and used in the oceanic models. The subskin temperature observed by the passive microwave observations differ from the temperature at 1 m, by up to a few degrees during the day under high insulation and low wind speed [see *Donlon et al.*, 2002]. Note that the IR observations measure the skin temperature ( $\sim 0.01$  mm) that is usually slightly colder than the subskin temperature measured by the microwaves. These differences have to be accounted for when merging estimates from different sources. Usually, the microwave SST algorithms are tuned to reproduce the temperature at 1 m, as the subskin temperature is not measured in situ.

[5] SST retrieval from passive microwaves has been tested early with the advent of the scanning multichannel microwave radiometer onboard Seasat and Nimbus 7 in 1978, with dual polarization channels at 6.6, 10.7, 18, 21, and 37 GHz [*Wilheit and Chang*, 1980]. The SST was retrieved with a spatial resolution of 150 km, at local noon and midnight, to within  $-0.14 \pm 1.1$  K onboard Seasat [*Robinson*, 1995]. However, calibration problems were noticed on Nimbus 7, and the SST products were not used operationally [*Milman and Wilheit*, 1985]. In 1997, the Tropical Rainfall Measurement Mission (TRMM) Microwave Instrument (TMI) provided the first reliable satellite observations below 12 GHz, for the tropical regions between  $\pm 40^\circ$  in latitude. TMI has channels at 10.65, 19.35, 22.235, 37.0, and 85.5 GHz. The measurements have a 50 km spatial resolution, but are oversampled, making it possible to deliver SST products with a  $\sim 25$  km spatial resolution [*Wentz et al.*, 2000]. Since 2002, the Advanced Microwave Scanning Radiometer-E (AMSR-E) onboard Earth Observing System (EOS)-Aqua measures down to 6.9 GHz. Although equipped with channels sensitive to the SST (6.6 and 10.7 GHz), WindSat has not been intensively used for SST retrievals, likely because its main purpose was to test the full polarimetric capacity for wind vector retrieval and because it is less available operationally (it is a U.S. navy mission).

[6] To our knowledge, most microwave-derived SST studies, from TMI or from AMSR-E, are based on retrievals from *Wentz and colleagues* [e.g., *Wentz et al.*, 2000; *Gentemann et al.*, 2010a]. The algorithm is based on radiative transfer (RT) simulations on a large data set of atmospheric/oceanic conditions. The resulting simulated

brightness temperatures are used to train a two-stage multi-regression algorithm. First, the SST and ocean wind speed (OWS) are estimated, using all available channels from the given radiometer. Then, localized algorithms (i.e., for special ranges of SST  $\pm 1.5^\circ$  and wind speed  $\pm 1.5$  m/s) are developed (1444 total) to account for nonlinearities in the relationship between SST and the brightness temperatures ( $TB_s$ ). Fine tunings are further applied to agree with the Reynolds product. The SST algorithms have been carefully evaluated by comparison with in situ measurements (ships, buoys) and IR satellite estimates [e.g., *Stammer et al.*, 2003; *Ricciardulli and Wentz*, 2004; *Castro et al.*, 2008; *O'Carroll et al.*, 2008]. Rainy pixels are excluded from the comparisons (using the simultaneous 37 GHz observations of TMI or AMSR-E). The microwave SSTs provide almost all-weather estimates, with, for instance, 78% daily coverage with TMI over Western Pacific and Eastern India in a year, compared to 48% with AVHRR [*Guan and Kawumara*, 2003]. *Gentemann et al.* [2010b] estimate the accuracy of the SST retrieval when suppressing the lower frequency observations around 6 GHz for future mission consideration.

[7] The biases between microwave SST and IR or in situ estimates are limited (below  $0.1^\circ\text{C}$ ) with standard deviation (StD) of  $\sim 0.5^\circ$ , for both TMI and AMSR-E [e.g., *Chelton and Wentz*, 2005]. Part of these differences is related to time and space mismatches, errors in the in situ or IR estimates, and differences in measurement depths. A large number of studies concentrated on the tropical ocean, using TMI observations [e.g., *Guan and Kawumara*, 2003]. However, the algorithms have also been tested at high latitudes [e.g., *Dong et al.*, 2006]. Differences have been systematically analyzed with respect to many factors, such as wind speed, total columnar water vapor (TCWV), cloud water, location, local temperature, or local time. The sensitivity to wind speed is the dominant effect. Accuracy is lower for wind speed above 12 m/s, partly related to the difficulty of the models to account for the presence of foam [*Dong et al.*, 2006]. A warm bias is also observed with respect to buoys, during the day under low wind conditions, due to the difference between the measurement depths of the two instruments. To enhance the SST retrieval accuracy, it is important to have the OWS measured simultaneously. The sensitivity of the SST retrieval to TCWV has also been evaluated and is more important than expected: it could be related to other parameters that are coincidentally correlated to water vapor [*Castro et al.*, 2008]. Simultaneous microwave observations in water vapor sensitive channels (22 GHz for instance) provide the required information to correct for this effect. With respect to in situ measurements or IR satellite estimates, the microwave SST are systematically warm-biased close to coast (50–100 km), due to the contamination of the antenna field-of-view by the land. In addition, at high latitudes, ice contamination in the field of view has to be detected. Higher-frequency channels (85 GHz for instance) benefit from improved spatial resolution and could help provide SST information closer to the coast or ice.

[8] Blending of the SST data (in situ, IR, and microwaves) has been suggested within the Global Ocean Data Assimilation Experiment (GODAE) High Resolution

SST (GHRSSST, <http://www.ghrsst.org>), initiated in 2000 [see Donlon *et al.*, 2004, 2007]. It evolved very quickly from an experiment to routine products used operationally. GHRSSST has led to the development of daily SST analysis (the UK Met Office OSTIA system for instance). In order to offer accurate merged products, the users need to be aware of the limitation of each SST source and to account for it. As a consequence, the accuracy of the microwave product has to be specified, including its dependency to the other variables such as wind speed.

[9] To provide the user community with all-weather estimates of the SSTs that satisfy their requirements, i.e., with a  $\sim 10$  km spatial resolution and an accuracy of the order of 0.3 K globally, new missions have to be designed. The objective of this study is first to carefully analyze the potential of the microwave frequencies to provide the SST with the desired spatial and radiometric resolutions, taking into account the physical sensitivities as well as the technological constraints (e.g., available bandwidth for passive remote sensing, instrument noise, antenna size), and second, to propose instrument concepts for a microsatellite mission. The work formed part of a European Space Agency (ESA) study called MICROWAT (<http://www.microwat.org>) to study new mission concepts for passive microwave instruments. First, the data sets and tools used in this study are presented (section 2). A quick analysis of the SST temporal variability is presented to compare with the accuracy of the requested SST estimates. Second, a classic information content analysis is conducted, based on the calculation of the Jacobians (section 3). In order to provide a more realistic estimation of the potential of different frequency bands, full retrieval algorithms are developed under different instrument configurations, using a simulated training database (section 4). These retrievals are evaluated using AMSR-E observations and coincident buoy measurements. Based on the information content analysis and on the retrieval tests on real observations, new mission concepts are proposed to satisfy the user needs for SST mapping (section 5). Conclusions are provided in section 6.

## 2. Data Sets and the RT Model

[10] The analysis of the sensitivity of the satellite observations is based on a simulated data set, calculated from surface and atmospheric information derived from the European Center for Medium Range Forecasting (ECMWF) and coupled to the community RT code RTTOV.

[11] AMSR-E observations cover well the microwave frequencies that are suitable for SST estimations. Lower frequencies would be too sensitive to salinity, and higher frequencies would be too much affected by water vapor and clouds. Theoretically, other frequency bands could be adopted between 5 and 19 GHz, but within this frequency range, the sensitivity to the key parameters, namely the SST, the OWS, and the TCWV, varies smoothly [Wilheit *et al.*, 1980]. The selection of a specific band is essentially governed by the frequency allocation and spectrum protection related to passive observations, in order to avoid radio frequency interferences (RFI) as much as possible (see the International Telecommunication Union (ITU) Radio Regulation (RR) at <http://www.itu.int/pub/R-REG-RR-2008>). The only protected bands are the 6.425–7.250 GHz band

(protected but shared with fixed, and fixed-to-satellite links), the 10.600–10.700 GHz band (shared with fixed systems but with threshold defined, with only 10.680–10.700 GHz fully protected), the 15.350–15.400 GHz band (fully protected but very narrow so providing limited radiometric sensitivity), the 18.600–18.800 GHz (protected but shared with fixed, and fixed-to-satellite links). As a consequence, the simulations will be conducted at AMSR-E frequencies, for possible evaluation with real satellite observations and buoys.

## 2.1. Ocean and Atmospheric Information

### 2.1.1. European Centre for Medium-Range Weather Forecast Analysis

[12] The ocean surface properties and the atmospheric profiles are extracted from the six hourly operational global analyses from the Integrated Forecasting System (IFS) of the ECMWF, for a full year (2008), with a spatial resolution of  $1.125^\circ \times 1.125^\circ$ . In order to run accurate RT simulations, the following information are kept: the temperature, water vapour, and ozone profiles on 43 pressure levels ranging from 1000 to 1 hPa (these levels are interpolated from the original 21 levels in order to be used with the RT code described below) and for the surface, the SST, the 10 m horizontal wind, and the 2 m pressure and temperature. Cloud information is also provided. Their contribution is calculated as well, but neglecting their scattering effect (this is justified by the emphasis of our analysis on the lower microwave frequencies that are not affected by hydrometeor scattering). About 800,000 profiles are used for the training of the algorithm.

[13] From the ECMWF analysis, the temporal variability of the SST is limited. Figure 1 represents the mean and the StD of the SST for each location of the ocean, for the month of January and July, as calculated from 2007 to 2010. For most regions, the StD is below 1 K, reinforcing the requirement for accurate SST measurements in order to possibly capture these limited variations.

### 2.1.2. National Oceanic and Atmospheric Administration Buoys

[14] The NOAA buoy information will help evaluate the SST retrieval from satellite observations. Data from two buoy networks have been collected, from 1997 to 2010, one from the Tropical Atmosphere Ocean (TAO) project (<http://www.pmel.noaa.gov/tao>) and the other from the Prediction and Research Moored Array in the Atlantic (PIRATA) (<http://www.pmel.noaa.gov/pirata>). They also provide an estimate of SST temporal variability at local scale. Table 2 gives the mean variability as well as its StD for SST and OWS, depending on the temporal sampling of the buoys. As expected, in situ point measurements show more variability than analysis averaged over large areas, especially when they are sampled at a high temporal rate. However, note again that the temporal variability is still limited, emphasizing the need for accurate satellite estimates of SST to detect these variations.

## 2.2. AMSR-E Observations

[15] AMSR-E onboard the EOS-Aqua satellite scans the Earth with a constant incidence angle ( $55^\circ$ ) at six frequencies between 6.9 and 89.0 GHz for both orthogonal polarizations. The spatial resolution ranges from  $74 \text{ km} \times 43 \text{ km}$

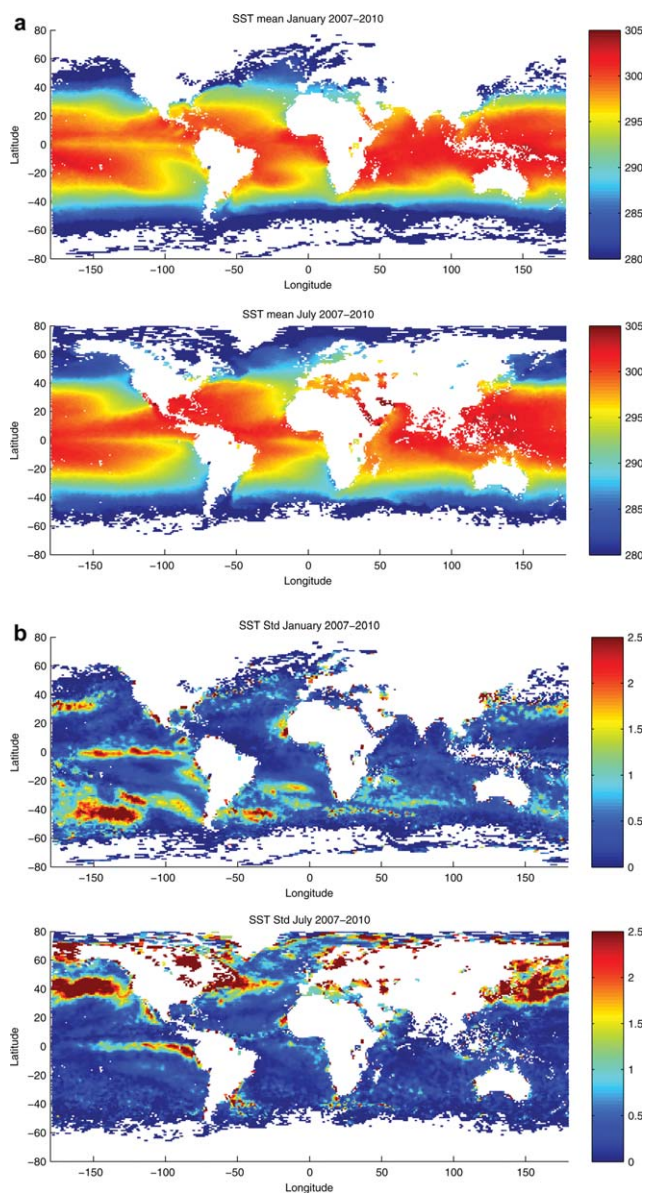


**Figure 1.** (left) Mean and (right) StD of the SST from the ECMWF analysis for the months of (top) January and (bottom) July from 2007 to 2010.

at 6.9 GHz to 6 km × 4 km at 89 GHz. The radiometric sensitivity of the instrument is indicated on Table 3 for all channels, along with the main instrument characteristics. Its equator crossing times are 13:30 and 01:30 local time.

### 2.3. Radiative Transfer Model RTTOV

[16] The RTTOV model has been developed for very rapid calculations of radiances in the infrared and microwaves, primarily for use in variational assimilation of satellite observations within NWP centers [Saunders *et al.*, 1999]. It is jointly developed by the UK Meteorological Office, Météo-France, and ECMWF in the framework of EUMETSAT-funded NWP Satellite Application Facility and also other EUMETSAT-sponsored activities. The original code was described by Eyre and Woolf [1988]. *Matri-*

**Table 2.** Temporal SST Variability of the NOAA Buoys as a Function of Temporal Resolution<sup>a</sup>

Temporal Sampling	SST Variability		
	Mean (K)	StD (K)	Buoy Number
$x < 15$ mn	1.68	0.63	87
$15 \text{ mn} \leq x < 60$ mn	1.04	0.55	78
$60 \text{ mn} \leq x$	0.91	0.53	39

<sup>a</sup>The mean corresponds to the mean of the standard deviation, calculated for each buoy individually. Same for the Std, calculated as the standard of the individual standard deviation of the different buoys.

*cardi et al.* [2004] presents more recent developments. Over ocean, the emissivities are computed by the FASTEM-3 model [Deblonde and English, 2001]. FASTEM-3 uses a two-scale ocean roughness approximation. The emission from large-scale waves is modeled by the geometric optics: the large-scale waves are modeled by tilting surface facets, each facet satisfying the specular reflection condition and the slope distribution being described by an ocean surface spectrum. Nonspecular scattering from the small-scale waves is added. The ocean permittivity is derived from Ellison *et al.* [1998] and the foam coverage calculated from Monahan and Muircheartaigh [1986], with an emissivity of one. A more recent version of FASTEM is now available (FASTEM-4) [Liu *et al.*, 2011]. In terms of sensitivity to SST, changes from FASTEM-3 to 4 are limited, as mentioned by Liu *et al.* [2011] in the conclusion of the paper. To our knowledge, at low frequencies, their differences have not been documented yet with respect to real observations. Tests are currently under way at NOAA for these frequencies (Liu, personal communication).

## 3. Information Content Analysis

### 3.1. Methodology

[17] In order to test the information content of the instrument configurations considered in this study, we use the classic information content analysis [Rodgers, 1976, 1990]. In this approach, the RT is linearized around a first guess solution:

$$(TB_{\epsilon} - TB_0) = A \cdot (f - f_0) + \epsilon, \quad (1)$$

where  $f$  are the geophysical variables (SST, OWS, and the water vapor profile in our case),  $f_0$  is a first guess of these variables,  $TB_{\epsilon}$  is the brightness temperatures observed by the microwave instrument,  $TB_0$  is the brightness temperatures corresponding to the first guess solution,  $A$  is the

**Table 3.** AMSR-E Instrument Performance Characteristics (Center Frequency, Bandwidth, Accuracy, and the Spatial Resolution Is Characterized Using the Field of View (FOV))

Frequency (GHz)	6.925	10.65	18.7	23.8	36.5	89.0
BW (MHz)	350	100	200	400	1000	3000
Radiometric sensitivity (K)	0.30	0.60	0.60	0.60	0.60	1.10
FOV (km × km)	74 × 43	51 × 30	27 × 16	31 × 18	14 × 8	6 × 4

Jacobian of the RT model, and  $\epsilon$  the instrument noise (other sources of uncertainties can also be included in this term). We will only retrieve the SST and OWS. The water vapor profile is not retrieved but appears in the equation to account for its uncertainties in the following information content analysis. If the hypothesis that the variables considered in the problem are Gaussian is valid, the Bayesian retrieval can be estimated using an iterative procedure:

$$f = f_0 + (A^t \cdot S_\epsilon^{-1} \cdot A + S_f^{-1})^{-1} \cdot A^t \cdot S_\epsilon^{-1} \cdot (TB_\epsilon - TB_0), \quad (2)$$

where  $S_\epsilon$  is the covariance of the instrument noise and  $S_f$  is the covariance matrix of the first guess error. This is the traditional retrieval method used in NWP centers. It is always very important to have an error estimate associated to the retrievals. In the retrieval method of equation (2), the error on the retrieval is given by the retrieval error covariance matrix:

$$Q = (A^t \cdot S_\epsilon^{-1} \cdot A + S_f^{-1})^{-1}. \quad (3)$$

[18] It is then possible to use this expression to measure the accuracy of retrievals based on the instrument noise information, on the Jacobian of the RT for the particular channels that are considered, and on the a priori information provided by the first guess. In the following sections, various instrumental configurations will be tested (channel number and frequencies, instrument noises), and the retrieval error covariance matrix  $Q$  will be estimated each time. For operational meteorological applications, the accuracy is the root-mean-square (r.m.s.) difference between the actual measurement and the truth, inclusive of random errors and bias [Stammer *et al.*, 2007]. Note that the information content analysis cannot account for systematic error (bias) but only for random errors.

### 3.2. Results

[19] The first piece of information required in the expression of equation (3) is  $S_f$ , the covariance matrix of the first guess error. This represents the error of the a priori information (before the inversion). In our calculations, the StD of the a priori information are 3.31 K for the SST, 1.33 m/s for the OWS, and 10% in water vapor profile on each level. The first guess error on OWS is rather optimistic with respect to ECMWF OWS precision at local scale, but it is envisaged to fly the MICROWAT in a “train” mode with other satellite missions providing additional information on OWS. In Figure 2, the associated correlation matrix is represented for a state variable composed of the SST, the OWS, and 43 atmospheric humidity levels (from the top-of-the-atmosphere down to the surface), as extracted from the ECMWF database. The SST and the TCWV close to the surface are well correlated, with decreasing correlation with increasing altitude, as expected. The OWS is not correlated to other variables, meaning that the correlation between variables cannot be exploited for the retrieval of the OWS. Note that these results are global: for specific regions, other correlations could be found, and if region-dependent algorithms were to be developed, these relationships could be exploited.

[20] Another piece of information is the linearization  $A$  of the RT. In Figure 3, the sensitivity of the AMSR-E chan-

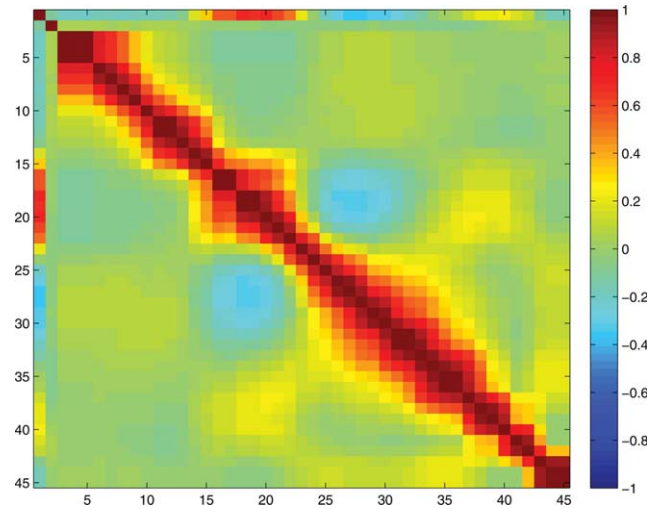


**Figure 2.** Correlation matrix for the first guess errors. Variable 1 is the SST, variable 2 is the OWS, and variables 3–45 are the atmospheric water vapor from the top of the atmosphere to the surface.

nels to SST is provided for different types of situations, in terms of OWS, TCWV, and SST (the same midlatitude atmosphere is used for the simulations, scaled to match the desired water vapor integrated content). Most of the time, for a given frequency, the sensitivity to the SST ( $\partial TB / \partial SST$ ) is higher for the vertical polarization than for the horizontal one: this is simply related to the larger emissivity in vertical polarization as compared to the horizontal one. Note that at frequencies above 15 GHz, the sensitivity to the SST increases with SST, whereas at lower frequencies, the SST for which the sensitivity is optimum is around 295 K. As expected, the sensitivity of the lower channels to SST does not change with water vapor content. It does not vary much with wind speed either. However, a significant change in behavior is observed with SST, with the sensitivity at high frequencies rapidly decreasing for SSTs below 285 K. For high SSTs, the sensitivities are similar at 6 and 10 GHz; for lower SSTs, the sensitivities decrease considerably at 10 GHz with almost no sensitivity at all for temperature around 275 K. This is due to the sensitivity of the dielectric properties of the sea water to the SST: below  $\sim 8$  GHz, the real part of the permittivity is almost insensitive to the SST, whereas above this frequency, it decreases strongly with SST, with impact on the emissivity.

[21] Similar to Figure 3, Figure 4 presents the sensitivity of AMSR-E channels to OWS. The horizontal polarizations are more sensitive to the OWS than the vertical polarizations: the emission signal is lower due to a lower emissivity in H, and as a consequence, the reflected contribution is larger. The sensitivity to the OWS does not change much with frequency, except for humid atmospheres, in channels that are affected by water vapor such as the 23 and the 89 GHz channels. It does not change much with the SST either.

[22] The theoretical accuracy of the SST and OWS retrievals are calculated in Figure 5. The instrument noises correspond to the actual AMSR-E instrument (see Table 3). These estimations are performed using  $S_f$ , so the retrieval accuracy of OWS and SST includes the uncertainties in the

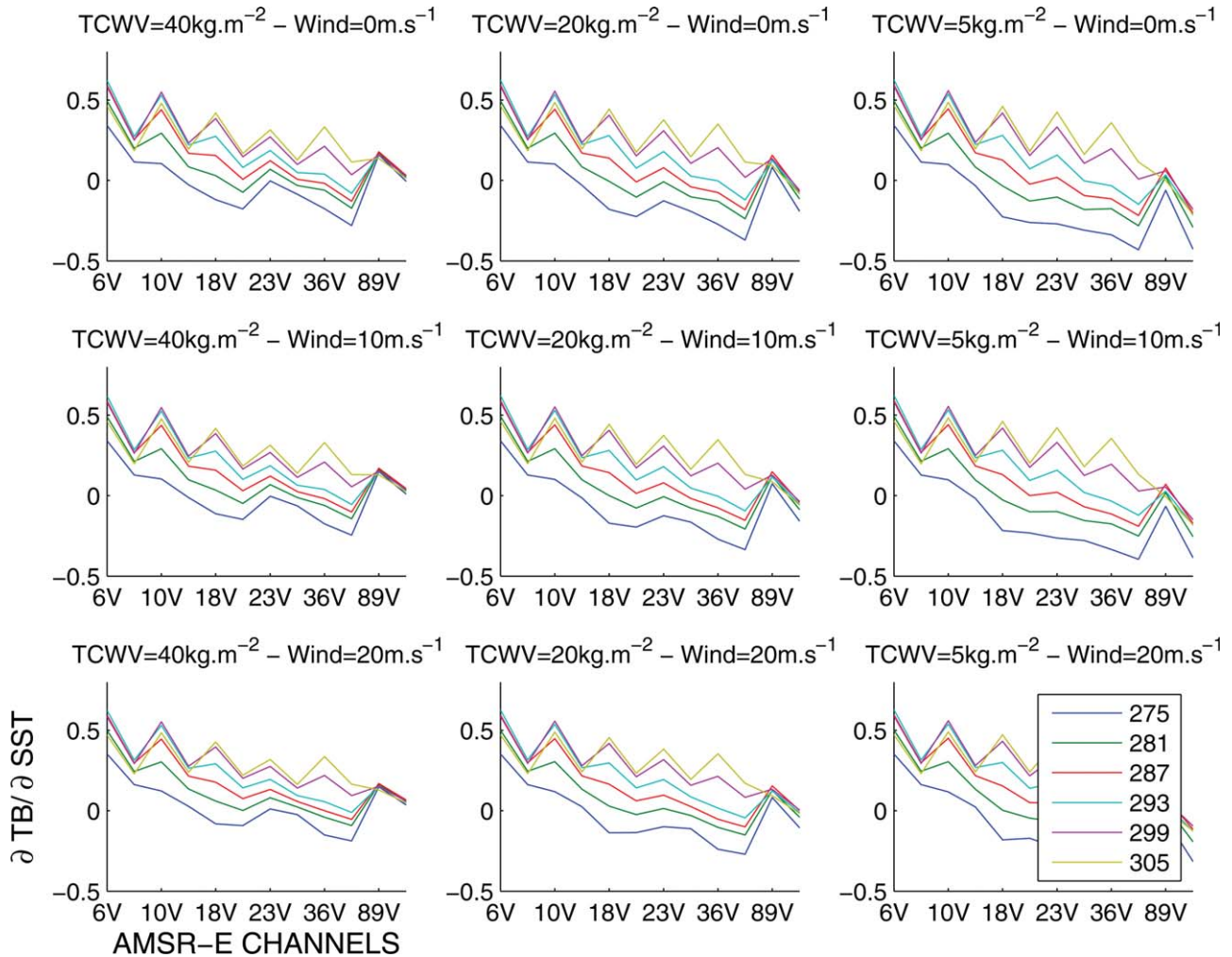


**Figure 3.** Sensitivity of the AMSR-E channels to the SST for different TCWV, OWS, and SSTs. On the horizontal axis, for each frequency, the vertical polarization is presented, then the horizontal one (the H polarization does not appear in the label for clarity purposes).

water vapor profile, but no other variable is taken into account. The accuracy fluctuates significantly from one situation to another, due to the difference between the Jacobians (Figures 3 and 4). This means that a reliable information content analysis requires computing statistics over a wide range of atmospheric and surface conditions. Generally speaking, the retrieval accuracy for both SST and OWS decreases with increasing atmospheric water vapor content (note that large water vapor contents for very low SSTs as in the top left figure are very unlikely to happen in the real world). The SST accuracy strongly fluctuates with SST, with a maximum accuracy around 295 K, which is in agreement with the maximum of the Jacobians at low frequencies for this range of SST (see Figure 3). The accuracy of the SST tends to decrease with increasing OWS. It is worth noting that only for the most optimal cases, the theoretical accuracy of the SST with AMSR-E does reach the accuracies sometimes claimed (e.g., 0.42 K in *O'Carroll et al.* [2008], or 0.41 K and 0.35 K for the TOGA and PIRATA buoys (1989–2005) in *Gentemann et al.* [2010a]). The accuracy of OWS increases almost linearly with increasing OWS, with a steeper slope for low

SSTs. The instrument noises as well as their relative values from a channel to the other play a key role in the retrieval accuracy. In order to test the impact of the instrument noise, accuracy estimates have also been calculated for a fixed noise of 0.3 K for all AMSR-E channels. The impact is significant, for all situations (not shown): this level of noise, and even better, can be realistically obtained by current day radiometer technology. The absence of 6 and 89 GHz channels has also been tested. Suppressing the lower frequency would make it possible a better spatial resolution for a given antenna size; on the other hand, suppressing the higher frequency would relax the constraint on the surface quality of a large antenna. As expected (not shown), the role of the higher frequency is limited for SST retrieval, but suppressing the low-frequency channel has a strong impact, especially under cold SST conditions.

#### 4. Retrieval Tests on Simulated Data Sets and Evaluation on Real Observations

[23] The information content analysis gives a preliminary indication of the importance of the different

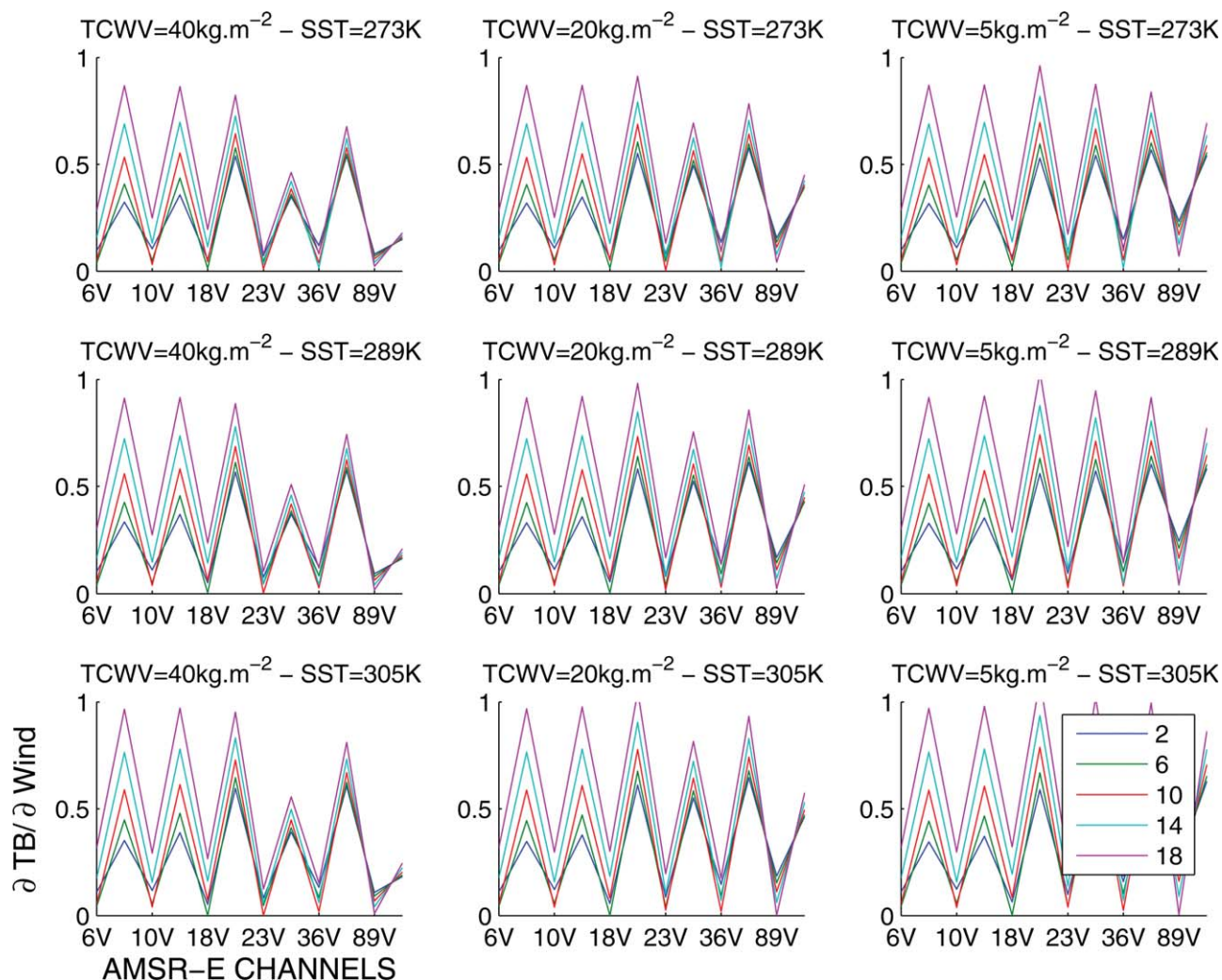


**Figure 4.** Same as previous figure, but for the sensitivity of the AMSR-E channels to the OWS.

characteristics of the instrument for the retrieval of the SST. However, in order to precisely assess the impact of the main instrument characteristics (frequency, noise), we develop inversion algorithms that provide a more realistic estimate of the retrieved accuracy at a global scale. With such an approach, the limitations of the traditional information content analysis resulting from simplistic assumptions (e.g., Gaussian character of the variables and uncertainties, linearization of the RT, first-guess errors similar for each surface condition) are avoided. A full retrieval scheme allows taking into account nonlinearities, saturation effect, and state dependence of the retrieval accuracies. The retrieval can be tested on a large and diverse set of situations. In addition, the retrieval can be evaluated on available satellite observations, with possible comparison with in situ buoy measurements.

#### 4.1. Development of a Neural Network Retrieval

[24] In order to test the information that can be extracted from satellite observations only, a neural network (NN) inversion scheme is developed in this study. It is a nonlinear regression tool that has been successfully used in many remote sensing applications [e.g., Aires *et al.*, 2011]. The Multi-Layered Perceptron (MLP) model [Rumelhart *et al.*,

1986] is selected here. It is a nonlinear mapping model: given an input (the microwave satellite measurements), it provides an output (the geophysical variables to retrieve, i.e., the SST) in a nonlinear way. The MLP model is defined by the number of input neurons (i.e., the number of channels), the number of outputs (i.e., the number of geophysical variables to retrieve), and the number of neurons in the hidden layers that controls the complexity of the model. In this paper, a NN model with only one hidden layer will be considered. A study has to be conducted to define the optimal number of neurons in the hidden layer: too many free parameters in the model can conduct to overlearning (overparameterization) leading to degraded generalization properties. On the contrary, too few free parameters will yield underparameterization and bias error in the model. The NN is a parametric model, and its parameters need to be estimated during a so-called training stage. A training database is first built. It includes samples of associated inputs (microwave observations) and outputs (SST). These samples have been extracted randomly from 1 year of ECMWF analysis and the associated RTTOV simulations of the satellite observations.

[25] The training database has been equalized in SST, in order to avoid penalizing the low SSTs that are statistically

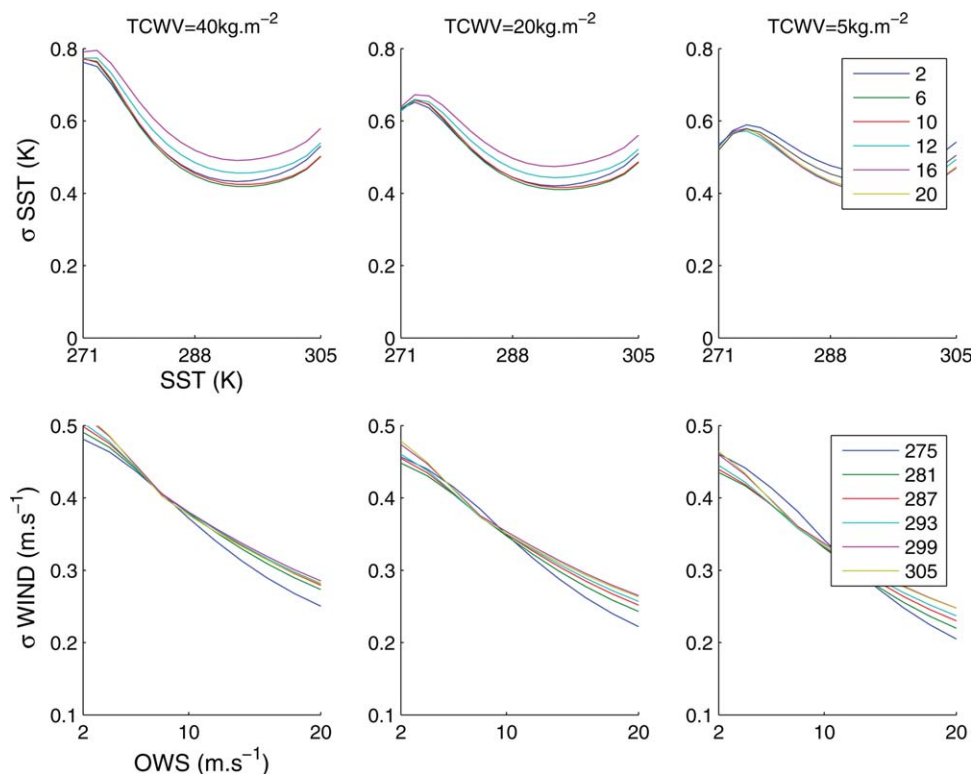


**Figure 5.** Retrieval accuracy estimated from information content analysis for the SST and OWS, for different conditions, in terms of TCWV, SST, and OWS. The present AMSR-E instrument noise is adopted (see Table 3).

less frequent at a global scale. This means that the same number of situations is considered for all SST bins between 273 and 303 K. Then, an optimization algorithm (the back-propagation) is used to evaluate the NN parameters that reduce the NN errors in the learning data set.

#### 4.2. Comparison of Different Instrumental Configurations in Simulated Data

[26] What is the minimum frequency selection that can provide SST retrieval with the required characteristics? The AMSR-E instrument serves several purposes but is not dedicated to the SST estimation, and as a consequence includes channels that are not necessary for SST retrieval. Here we test several channel selections in retrieval mode, based on the AMSR-E instrument.

[27] The requirement for high spatial resolution makes it necessary to have a large real aperture antenna or to develop an interferometric system. With real aperture antenna system, suppressing the lower frequency would make it possible to have a smaller antenna. With interferometric system, the idea is to use only a limited number of frequencies, the number of necessary receivers per frequency being large.

[28] As shown before, the 6 GHz provides a good sensitivity to the SST, over a large range of SST including cold ones, but requires large antenna to provide the necessary spatial resolution. The available bandwidth around the 6 GHz makes it possible to reach good radiometric sensitivity, contrary to the 11 GHz, where the possible receiver bandwidth is limited due to frequency-allocation problems.

Suppressing the 89 GHz channel will avoid the use of an antenna of high-quality surface: this is very interesting when large reflectors are necessary to obtain a high spatial resolution at low frequencies.

[29] Table 4 summarizes the results of the SST inversion algorithms for different channel selections: with all the channels, and when suppressing the lower and higher frequency channels. The results stress the interest of the 6 GHz channels for SST estimation, with a doubling of the SST errors when the 6 GHz channel is suppressed (from a RMS of 0.43–0.89 K). They also clearly show that the 89 GHz channels do not bring much information in terms of SST, with very similar theoretical results observed with and without these channels (RMS from 0.43 to 0.44 K, respectively, with and without the 89 GHz channels). For a simple instrument configuration, different combinations of frequencies have been tested (they are not all shown here). A test has been performed with only two frequencies, 6 and 18 GHz with both polarizations for each frequency. The increase in SST error is rather limited (from 0.43 to 0.55 K) given the huge simplification that would be introduced on the instrument design.

[30] In order to assess the noise impact, a uniform noise is tested, at 0.1 K on all AMSR-E channels. This corresponds to the noise specified by *Wentz and Meissner* [2000] and by *Gentemann et al.* [2010b] in their estimations. It is used here for comparison purposes with the results provided in *Gentemann et al.* [2010a, 2010b]. Although very optimistic, this noise figure does not jeopardize the quality of the *Gentemann et al.* SST retrieval,

**Table 4.** Error Estimation for SST From the Inversion Algorithm Using AMSR-E Frequencies Using Simulated Measurements: First With the Real AMSR-E Noise (Table 3), and Then With a Fixed 0.1 K Noise for All Channels<sup>a</sup>

	SST Retrieval Error Estimates (K)		
	$\bar{x}$	$\sigma$	RMS
AMSR-E Noise Given in Table 3			
111111111111	0.00	0.43	0.43
001111111111	-0.02	0.89	0.89
111111111100	0.00	0.44	0.44
110011000000	0.00	0.55	0.55
AMSR-E Noise 0.1 K for All Channels			
111111111111	0.00	0.15	0.15

<sup>a</sup>The channels used in the retrieval are indicated with “1” and the channels that are suppressed are indicated with “0.”

given the way this information is used in their methodology. The importance of the instrument noise is clearly illustrated (Table 4), with a reduction of the SST error to 0.15 K, as compared to 0.43 K (all channels being used).

[31] Figure 6 presents the RMS errors of SST retrieval as a function of SST, with all AMSR-E channels, with only the 6 and 18 GHz AMSR-E channels, and with all AMSR-E channels except the 6 GHz. Without the 6 GHz, the retrieval errors are very large for low SST, as expected from the information content analysis. However, a simple instrument with two frequencies including the 6 GHz (both polarizations for each one) provides accurate SST retrieval regardless of the SST range. The histogram of the SST in the initial database (in percentage of the population) is also indicated. Note that as specified before, the training data set has been “equalized” in SST (i.e., the same number of situations per SST range), to avoid favoring a SST range in the retrieval.

[32] All these results tend to prove that a low noise instrument with a limited number of channels including the 6 GHz could satisfy the user requirements in terms of SST, all over the globe.

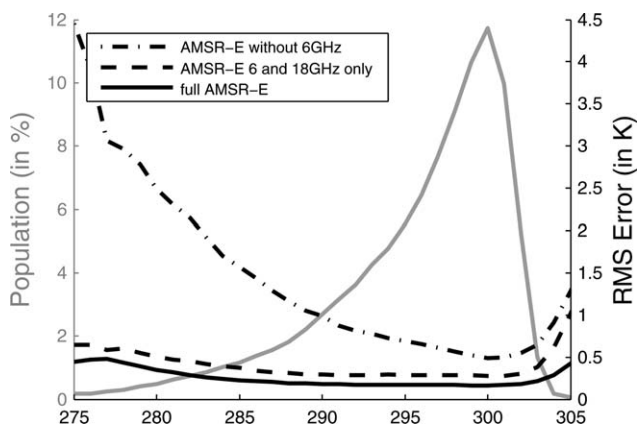


**Figure 6.** Theoretical RMS errors of the SST as a function of the SST, with all AMSR-E channels, with only the 6 and 18 GHz AMSR-E channels, and with all AMSR-E channels except the 6 GHz. The histogram of the SST in the initial database (in percentage of the population) is also indicated.

**Table 5.** Comparisons Between SST AMSR-E Retrievals and Buoy Measurements, Using First All Channels and Then a Subset of Channels<sup>a</sup>

	Buoy Departure in SST (K)		
	$\bar{x}$	$\sigma$	RMS
Analysis	0.18	0.39	0.43
111111111111	-0.02	0.67	0.67
001111111111	-0.03	0.72	0.72
110011000000	0.03	0.67	0.67

<sup>a</sup>The departure between ECMWF analysis and the buoys is also indicated.

### 4.3. Evaluation of the Different Instrumental Configurations With Real Observations

[33] To check the consistency of our theoretical results, the retrieval algorithms have been tested using real observations and compared to buoy measurements, first using all the channels, then using only channel selections (Table 5). The statistical results are presented for September 2002 and January 2003, over the tropical region. The cloudy cases are kept, but precipitations are filtered out, using the flag from the ECMWF analysis as well as the information from the buoys. The analyses are interpolated to the buoy locations. The buoy measurements are averaged over a 2 h window centered on the satellite overpassing time. As expected, the departures from the buoy measurements are larger than the theoretical retrieval errors. The errors in the buoy measurements and the coincidence errors (in space and time) are included in these statistics in addition to the actual retrieval accuracy. However, the same trend is observed between the configurations, with the lack of low-frequency channel degrading the retrieval performances, but in a more limited proportion than in theory. The departure between the buoy measurements and the analyses has also been calculated: it provides an estimate of the expected difference between point measurement and large-scale estimates. The retrieval seems to be less accurate than the analysis: this is due to the fact that the analysis already assimilates the buoy measurements. Note that the retrieval accuracy obtained here is lower than what can be found in the literature. First, our NN inversion algorithm is a “global” retrieval scheme contrary to “local” inversions (as in *Wentz et al.* [2000], for instance): a local inversion is designed to perform on very specific conditions and therefore, it is generally more accurate than global retrieval models that perform on all cases. Second, our retrieval scheme has not been calibrated a posteriori using in situ buoy measurements. The objective of our retrieval experiment is to assess the information that can be extracted from satellite observations only. It is not to optimize the retrieval of SST using all forms of available information and technics.

## 5. Definition of New Mission Concepts

[34] The previous analyses showed that the low-frequency channels are very important in determining accurate SSTs. Despite their limitations in terms of spatial resolution, measurements at frequencies around 6 GHz cannot be avoided, given first their potentially larger

**Table 6.** Characteristics of the Three Different New Instrument Concepts

	Frequency (GHz)	Bandwidth (MHz)	Radiometric Sensitivity (K)	Spatial Resolution (km)	Receiver Number	Mass(kg)	Power (W)
Real aperture antenna	6.9 (V+H)	825	0.12	15	16	300	500
	18.7 (V+H)	200	0.26	15			
Interferometer	6.9 (V)	825	3.86	15	788	600	2500
2-D geometry	18.7 (V+H)	200	2.50	15	510	600	1000
Interferometer	6.9 (V)	30	0.14	15			
1-D geometry	18.7 (V+H)	80	0.37	15			

bandwidth (and consequently lower instrument noise) and second their higher sensitivity to low SSTs, both as compared to the 10 GHz channels. The analyses also emphasized the importance of low-noise receivers, with the SST retrieval accuracy related to the instrument accuracy. Two instrument concepts have been analyzed for a microsatellite, within the ESA MICROWAT study [Orlhac *et al.*, 2012]. The first concept suggests a real aperture antenna and the second one synthetic aperture antennas. A limited number of channels makes possible a synthetic aperture concept (antenna array complexity is acceptable for a dual-frequency instrument), and in the case of real antenna scheme, it facilitates the pixel duplication (to reduce the antenna rotation speed and improve the radiometric sensitivity). Due to the low frequency of the channels and the risk of RFI disturbance, RFI detection and mitigation hardware is proposed for all concepts. The incidence angle is  $53^\circ \pm 1.5^\circ$ . The performance of the two solutions is carefully evaluated, with current state-of-the-art technologies.

### 5.1. Real Aperture Antenna Concept

[35] This concept is based on a conical scanner and uses a rotating reflector and feed connected to the receivers. The preliminary design shows that a 9 m diameter reflector is necessary to achieve 10 km of across track footprint, but that requires a pliable reflector technology. A 6 m antenna provides 15 km footprint. A four-channel radiometer is proposed: 6.9 and 18.7 GHz for both V and H polarizations. The main performances being the radiometric resolution, the pixel duplication technique is adopted to improve the integration time, thanks to a reduction of antenna rotation speed. The rotation speed reduction also facilitates momentum compensation. A matrix of four pixels is proposed for each channel: this implies four receivers for each channel, i.e., a total of 16 receivers for the four channels. The radiometric resolution is 0.12 K at 6.9 GHz and 0.26 K at 18.7 GHz with four pixel duplication (with an antenna rotation speed of 6.6 RPM). Moreover, the instrument will perform fore and aft observations (note that the double view of the instrument is not accounted for in the calculation of the noise, i.e., the noise figure does not assume that the fore and aft views are averaged). The power consumption is estimated at 500 W. The rotating large reflector and the associated momentum compensation is a technical issue for this concept.

[36] Table 6 indicates the main instrument characteristics, and Figure 7 shows a potential satellite configuration for such a mission.

### 5.2. Synthetic Aperture Concept

[37] Two synthetic aperture concepts have been studied. A 2-D MIRAS SMOS-like instrument [Kerr *et al.*, 2001]

and a 1-D ESTAR-like instrument. The 2-D version leads to a huge number of antennas and receivers with an unrealistic power consumption and complexity. An estimation of close to 800 antennas would be needed. The 2-D image will only be used around  $53^\circ$  to obtain the required wind sensitivity. For the SST estimate, it might be possible to exploit the multiangular polarized information, and to avoid the use of two frequencies. However, based on the SMOS experiment, it appears very difficult to reach very low noise measurements with such a system. With a 3.9 K sensitivity on each measurement (see Table 6), more than 650 measurements would have to be averaged to reach a sensitivity of 0.15 K, which is clearly not feasible. A 1-D version has also been evaluated to reduce the number of antennas and receivers. To achieve a radiometric resolution of 0.15 K at 6.9 GHz and 0.35 K at 18.7 GHz, 150 antennas at 6.9 GHz (V only), and 180 antennas at 18.7 GHz are required for each polarization, for a total of 510 antennas. The antenna array at 6.9 GHz needs to be foldable. This feature could be complex because of the feeder system (not a simple reflector).

[38] Each element of the 1-D array will have a length of 6–8 m (depending on the final resolution required). The mass of such antenna could be extremely high and make the concept unrealistic. The power consumption has been

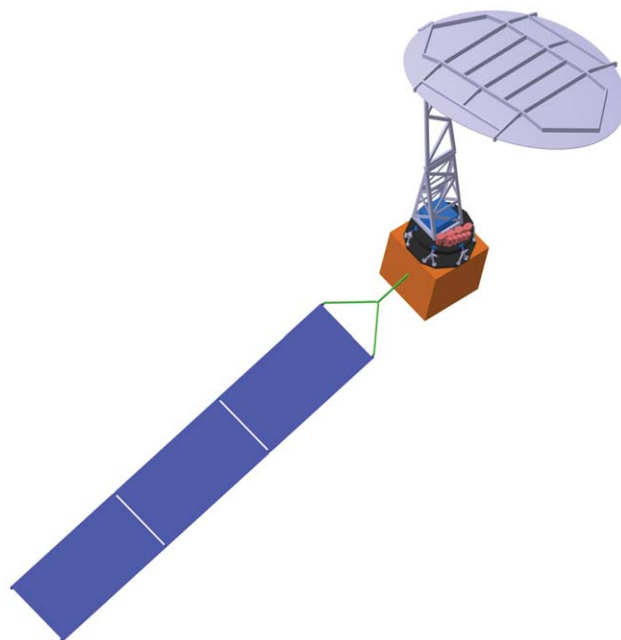


**Figure 7.** MICROWAT instrument concept with a real aperture antenna.

estimated above 2500 W for the 2-D concept and above 1000 W for the 1-D concept.

[39] The main disadvantage of the interferometer concept is the huge number of receivers (almost 800 antennas and receivers for the 2-D and 510 for the 1-D) that considerably increases the power consumption and can lead to an unrealistic instrument. Moreover, the radiometric resolution is limited by the fringe wash effect compared to the conical scanner. The fringe wash is due to the signal decorrelation introduced by the signal delay to reach all the antennas in the system: it depends on the array geometry, the view angle of the scene limit, and the bandwidth of the receivers. To limit this effect, note that the bandwidth is kept rather narrow as compared to the real aperture instrument case.

[40] Table 6 summarizes the main instrument characteristics for the new interferometric concepts, and Figure 8 presents a possible satellite configuration for a 1-D interferometer.

**5.3. Theoretical Error of Retrieval With Different Concepts**

[41] The retrieval accuracy has been estimated first using the information content methodology. The results are presented for the real aperture concept (Figure 9), similar to Figure 5. Major differences between the SST accuracy of the new instrument and AMSR-E are related to the low instrument noise of the new instrument, as compared to AMSR-E. Despite a much smaller number of frequency channels, the low instrument noise on the low-frequency channels of the new concept makes it possible to provide much better accuracy than with AMSR-E.

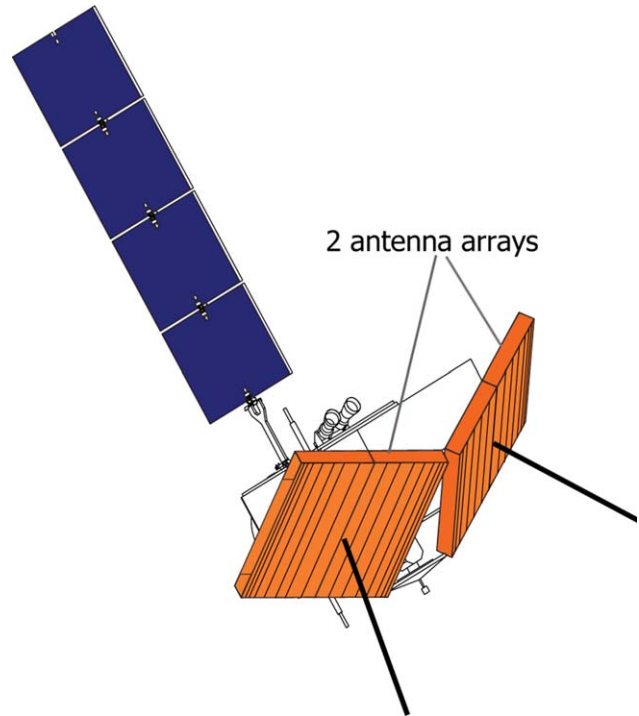


**Figure 8.** MICROWAT instrument concept with a 1-D interferometric antenna.

[42] For a more realistic estimate of the SST accuracy with the new instrument concept, retrieval algorithms have been developed for the three suggested instruments, using the NN inversion trained over ECMWF situations, as before

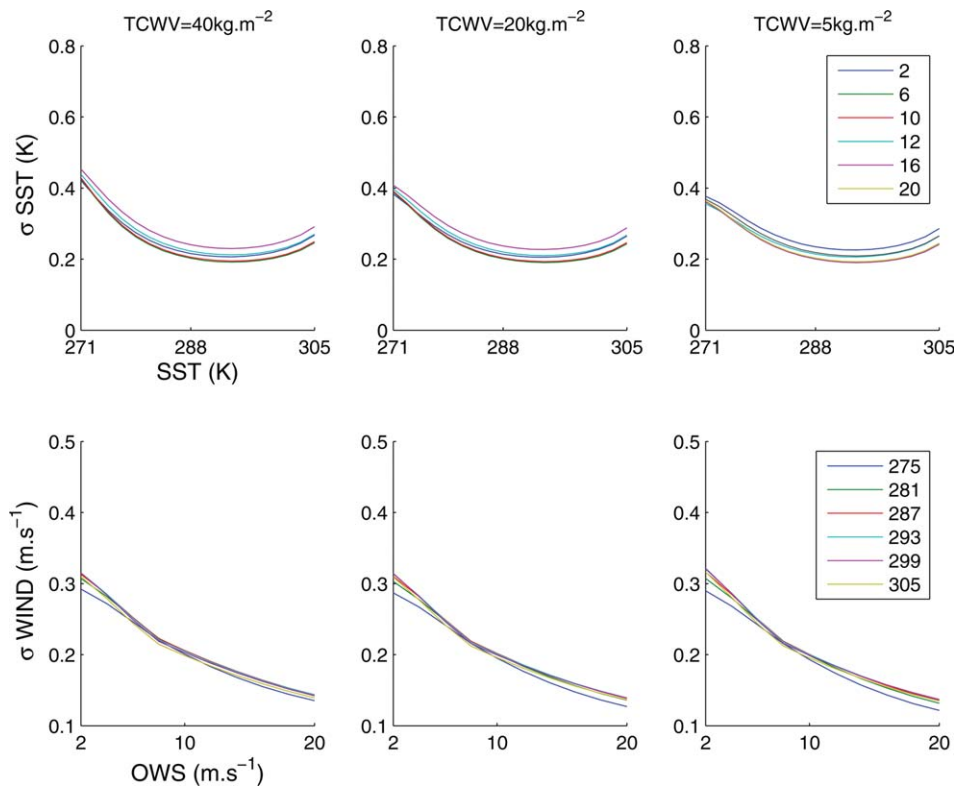


**Figure 9.** Retrieval accuracy estimated from information theory for SST and OWS, for different conditions, in terms of water vapor, SST, and OWS, for the new real aperture instrument (see Table 6).

**Table 7.** Error Estimation for SST From the Inversion Algorithm, for the Three Suggested Instrument Concepts

	SST Retrieval Error Estimates (K)		
	$\bar{x}$	$\sigma$	RMS
Real aperture antenna	0.00	0.32	0.32
Interferometer	0.02	1.27	1.27
2-D geometry			
Interferometer	0.00	0.38	0.38
1-D geometry			

with AMSR-E. The results are presented in Table 7. The 2-D interferometric system clearly does not meet the accuracy requirements, despite a very complex system with a huge number of antennas and receivers and high power consumption. The desired accuracy is obtained with the 1-D interferometric system, but with a high complexity (heavy instrument with 510 receivers and high power consumption). The conical scanner with a real aperture antenna provides the desired accuracy, with only two frequencies, thanks to the duplication of low-noise receivers. This is a significant improvement in the accuracy (from 0.43 K to 0.32 K), as compared to the performances obtained with AMSR-E, with a simple instrument providing 15 km spatial resolution SST.

## 6. Conclusions

[43] This study carefully analyzes the sensitivity of the microwave observations to the SST, with the objective of designing an optimized satellite instrument dedicated to an “all-weather” estimation of the SST at high spatial resolution (15 km).

[44] A retrieval algorithm is developed, trained on 1 year of ECMWF analysis coupled with RT calculations. Different frequency combinations are evaluated theoretically, and some of them are tested with real AMSR-E measurements, along with in situ buoy measurements. In order to really assess the information content of the satellite observations, the retrieval algorithms do not use any a priori information nor a posteriori calibration toward in situ observations.

[45] Our analysis underlines the importance of the low frequency observations around 6 GHz. Compared to the 11 GHz channel, the 6 GHz channel provides more sensitivity to the low SSTs and offers lower instrument noise, thanks to possibly broader channel bandwidths. However, it requires much larger antenna size for a given spatial resolution. Mission analysis has shown that the use of 6 GHz with adequate spatial resolution is feasible and the benefits outweigh the disadvantages. Our analysis also stresses the accuracy limits in the retrieval of SST: first, the SST retrieval accuracy is strongly constrained by the instrument noise level, second, uncertainties in the surface modeling as well as in other factors affecting the microwave signal (mainly wind speed, foam coverage, and emissivity) impact the SST retrieval accuracy.

[46] Two instrument concepts have been studied: one using classic real aperture antenna and the other using synthetic interferometric antennas. This analysis shows that 2-D interferometric systems would be very complex and would not satisfy the user requirements in terms of SST retrieval accuracy. A 1-D interferometric system could be proposed,

but its development requires additional investigation. A dedicated conical scanner onboard a microsatellite with a 6 m antenna and channels at 6.9 GHz (V and H) and 18.7 GHz (V and H) can provide SST retrieval accuracy of 0.3 K with a 15 km spatial resolution, with today’s technology, along with a good estimation of the surface wind speed.

[47] **Acknowledgments.** Financial support has been provided by European Space Agency “High Resolution Microwave Wind and Temperature (MICROWAT) Mission Concept Study,” contract 4500123573, 2010–2012. The authors are thankful to three anonymous reviewers for their constructive comments and suggestions. The authors are grateful to Bertrand Chapron for his careful reading of the manuscript.

## References

- Aires, F., M. Paul, C. Prigent, B. Rommen, and M. Bouvet (2011), Measure and exploitation of multisensor and multiwavelength synergy for remote sensing: 2. Application to the retrieval of atmospheric temperature and water vapor from MetOp, *J. Geophys. Res.*, *116*, D02302, doi:10.1029/2010JD014702.
- Castro, S. L., G. A. Wick, D. L. Jackson, and W. J. Emery (2008), Error characterization of infrared and microwave satellite sea surface temperature products for merging and analysis, *J. Geophys. Res.*, *113*, C03010, doi:10.1029/2006JC003829.
- Chelton, D. B., and F. J. Wentz (2005), Global microwave satellite observations of sea surface temperature for numerical weather prediction and climate research, *Bull. Am. Meteorol. Soc.*, *86*, 1097–1115.
- Deblonde, G., and S. English (2001), Evaluation of FASTEM and FASTEM-2, NWP SAF Report. [Available at <http://www.metoffice.com/research/interproj/nwpsaf/rtm/>].
- Dong, S., T. Gille, J. Sprintall, and C. L. Gentemann (2006), Validation of the advanced microwave scanning radiometer for the Earth Observing System (AMSR-E) sea surface temperature in the Southern Ocean, *J. Geophys. Res.*, *111*, C04002, doi:10.1029/2005JC002934.
- Donlon, C. J., P. J. Minnett, C. L. Gentemann, I. J. Barton, B. Ward, and J. Murray (2002), Towards improved validation of satellite sea surface skin temperature measurements for climate research, *J. Clim.*, *15*, 353–369.
- Donlon, C. J., L. Nykjaer, and C. L. Gentemann (2004), Using sea surface temperature measurements from microwave and infrared satellite measurements, *Int. J. Remote Sens.*, *25*, 1331–1336.
- Donlon, C. J., et al. (2007), The Global Ocean Data Assimilation Experiment (GODAE) high resolution sea surface temperature pilot project (GHRST-PP), *Bull. Am. Meteorol. Soc.*, *88*, 1197–1213.
- Ellison, W., A. Balana, G. Delbos, K. Lamkaouchi, L. Eymard, C. Guillou, and C. Prigent (1998), New permittivity measurements and interpolation functions for natural sea water, *Radio Sci.*, *33*, 668–685.
- Eyre, J. R., and H. M. Woolf (1988), Transmittance of atmospheric gases in the microwave region: A fast model, *Appl. Opt.*, *27*, 3244–3249.
- Gentemann, C. L., F. J. Wentz, M. Brewer, K. Hilburn, and D. Smith (2010a), *Passive microwave remote sensing of the ocean: An overview, in Oceanography From Space, Revisited*, edited by V. Barale, J. F. R. Gower, and L. Alberotanza, pp. 19–44, Springer, New York.
- Gentemann, C. L., T. Messner, and F. J. Wentz (2010b), Accuracy of satellite sea surface temperature at 7 and 11 GHz, *IEEE Trans. Geosci. Remote Sens.*, *48*, 1009–1018.
- Guan, L., and H. Kawamura (2003), SST availabilities of satellite infrared and microwave measurements, *J. Oceanogr.*, *59*, 201–209.
- Kerr, Y. H., P. Waldteufel, J.-P. Wigneron, J.-M. Martinuzzi, J. Font, and M. Berger (2001), Soil Moisture Retrieval from Space: The Soil Moisture and Ocean Salinity (SMOS) Mission, *IEEE Trans. Geosci. Remote Sens.*, *39*, 1729–1735.
- Liu, Q., F. Weng, and S. English (2011), An improved fast microwave water emissivity model, *IEEE Trans. Geosci. Remote Sens.*, *49*, 1238–1250.
- Matricardi, M., F. Chevallier, G. Kelly, and J.-N. Thepaut (2004), An improved general fast radiative transfer model for the assimilation of radiance observations, *Q. J. Roy. Meteorol. Soc.*, *30*, 153–173.
- Milman, A. S., and T. T. Wilheit (1985), Sea surface temperatures from the scanning multichannel microwave radiometer on Nimbus 7, *J. Geophys. Res.*, *90*(C6), 11,631–11,641.
- Monahan, E. C., and I. O. Muirchearthaigh (1986), Whitecaps and the passive remote sensing of the ocean surface, *Int. J. Remote Sens.*, *7*, 627–642.

- O'Carroll, A. G., J. R. Eyre, and R. W. Saunders (2008), Three-way error analysis between AATSR, AMSR-E, and in situ sea surface temperature observations, *J. Atmos. Oceanic Technol.*, *25*, 1197–2107.
- Orlhac, J.-C. (2012), Microwat ESA final report, Toulouse, France, EADS/Astrium, EF.RP.JCO.12.00081, Mar.
- Reul, N., S. Saux-Picart, B. Chapron, D. Vandemark, J. Tournadre, and J. Salisbury (2009), Demonstration of ocean surface salinity microwave measurements from space using AMSR-E data over the Amazon plume, *Geophys. Res. Lett.*, *36*, L13607, doi:10.1029/2009GL038860.
- Ricciardulli, L., and F. J. Wentz (2004), Uncertainties in sea surface retrievals from space: Comparison of microwave and infrared observations from TRMM, *J. Geophys. Res.*, *109*, C12013, doi:10.1029/2003JC002247.
- Robinson, I. S. (1995), *Satellite Oceanography: An Introduction for Oceanographers and Remote-Sensing Scientists*, Praxis Ser. in Remote Sens., 456 pp., John Wiley, New York.
- Rodgers, C. D. (1976), Retrieval of atmospheric temperature and composition from remote measurements of thermal radiation, *Rev. Geophys.*, *14*, 4, 609–624, doi:10.1029/RG014i004p00609.
- Rodgers, C. D. (1990), Characterization and error analysis of profiles retrieved from remote sounding measurements, *J. Geophys. Res.*, *95*(D5), 5587–5595.
- Rumelhart, D. E., G. E. Hinton, and R. J. Williams (1986), *Learning internal representations by error propagation*, in *Parallel Distributed Processing: Explorations in the Microstructure of Cognition*, vol. 1, *Foundations*, edited by D. E. Rumelhart, J. L. McClelland, and the PDP Research Group, pp. 318–362, MIT Press, Cambridge, Mass.
- Saunders, R. W., M. Matricardi, and P. Brunel (1999), An improved fast radiative transfer model for assimilation of satellite radiance observations, *Q. J. R. Meteorol. Soc.*, *125*, 1407–1425.
- Stammer, D., F. J. Wentz, and C. L. Gentemann (2003), Validation of microwave sea surface temperature measurements for climate purposes, *J. Clim.*, *16*, 73–87.
- Stammer, D., J. Johannesssen, P. LeTraon, P. Minnett, H. Roquet, and M. Srokosz (2007), Position paper: Requirements for ocean observations relevant to post-EPS, *AEG Ocean Topography and Ocean Imaging*, 10 Jan. 2007, Version 3.
- Wentz, F. J., C. L. Gentemann, D. K. Smith, and D. B. Chelton (2000), Satellite measurements of sea surface temperature through clouds, *Science*, *288*, 847–850.
- Wentz, F. J., T. Meissner (2000), AMSR Ocean Algorithm, Version 2, report number 121599A-1, Remote Sensing Systems, Santa Rosa, Calif., 66 pp.
- Wilheit, T. T., and A. T. C. Chang (1980), An algorithm for retrieval of ocean surface and atmospheric parameters from the observations of the scanning multichannel microwave radiometer, *Radio Sci.*, *15*, 525–544.
- Wilheit, T. T., A. T. C. Chang, and S. Milman (1980), Atmospheric corrections to passive microwave observations of the ocean, *Boundary Layer Meteorol.*, *18*, 65–77.